Spin and orbital magnetism of $FeBr_2$: a density functional theory study

2008 J. Phys.: Condens. Matter 20 025217

(http://iopscience.iop.org/0953-8984/20/2/025217)

J. Phys.: Condens. Matter **20** (2008) 025217 (5pp) doi:10.1088/0953-8984/20/02/025217

Spin and orbital magnetism of $FeBr_2$: a density functional theory study

Mahdi Sargolzaei[1] **and Ján Rusz**[2,3]

[1] Materials Research Laboratory (MRL), University of California, Santa Barbara, CA 93106, USA
[2] Department of Physics, Uppsala University, Box 530, S-751 21 Uppsala, Sweden
[3] Institute of Physics, Academy of Sciences of the Czech Republic, Na Slovance 2, CZ-182 21 Prague, Czech Republic

E-mail: mahdi@mrl.ucsb.edu

Received 10 August 2007, in final form 1 November 2007
Published 13 December 2007
Online at stacks.iop.org/JPhysCM/20/025217

Abstract
The electronic and magnetic properties of $FeBr_2$ have been studied in the framework of the local spin-density approximation (LSDA). In order to improve the intrinsic deficiency of the LSDA in describing orbital magnetism, two different orbital polarization corrections have been applied to Fe ions. The spin and orbital magnetic moments on the Fe and Br sites have been evaluated using the fully relativistic version of the full-potential local orbitals minimum basis method and the full-potential linearized augmented plane-wave + local orbitals method. We found a partially quenched orbital moment on the Fe ion and a small spin moment on the p states of the Br ion.

(Some figures in this article are in colour only in the electronic version)

1. Introduction

For several decades, intense experimental and theoretical efforts have been devoted to the investigation of electronic and magnetic properties of anhydrous dibromide of iron, $FeBr_2$, as an antiferromagnetic (AFM) insulator. $FeBr_2$ under an external field of 3.15 T, undergoes a magnetic phase transition from an antiferromagnetic phase to a paramagnetic phase with Néel temperature ($T_N = 14.2$ K) [1]. Due to its crystal and magnetic structure, it is also a very suitable candidate for comparing to the Ising model [2]. $FeBr_2$ is a well-known model system for the study of antiferromagnetism [3–5]. It adopts a hexagonal layer-type structure, which consists of layers of metal atoms separated by two layers of halide atoms. Neutron diffraction investigations show that the magnetic structure of $FeBr_2$ consists of ferromagnetic (FM) sheets of moments within the iron layers with magnetic moments oriented parallel to the hexagonal c axis [6]. The spin direction for the FM sheets alternates from layer to layer. Wilkinson *et al* emphasized that, within the experimental error, the magnetic moment on the Fe site ($4.4 \pm 0.7\ \mu_B$) is close to the atomic moments in which the orbital contribution is assumed to be quenched [6].

The trends witnessed here in the magnetic properties of $FeBr_2$ are the study of orbital magnetism in an antiferromagnetic insulator. The magnetic properties of magnetic materials are a combination of two order parameters, namely spin and orbital magnetic moments. Based on standard theoretical models, it is presupposed that ligand field interactions quench the orbital magnetic moment in 3d transition metals. Ropka *et al* [7] within their quasiatomic calculations, and later Youn *et al* [8] using an all-electron fully relativistic density functional method included by an intra-orbital correlation energy U on the d electrons, have shown that the orbital moment is indeed partially quenched by a ligand field in $FeBr_2$.

It is a well-known fact that the orbital moments of 3d transition metals calculated in the framework of the LSDA are usually underestimated by a factor of two [9]. In the present work we address two orbital polarization (OP) corrections in the LSDA. It is found that OP corrections predicted almost correctly the orbital moments of 3d transition ions. The paper is organized as follows: section 2 contains details of the crystal structure and the computational methods used, including the two OP corrections; section 3 presents the results and discussion (calculated spin moments and orbital moments), and, finally, the paper is summarized in section 4.

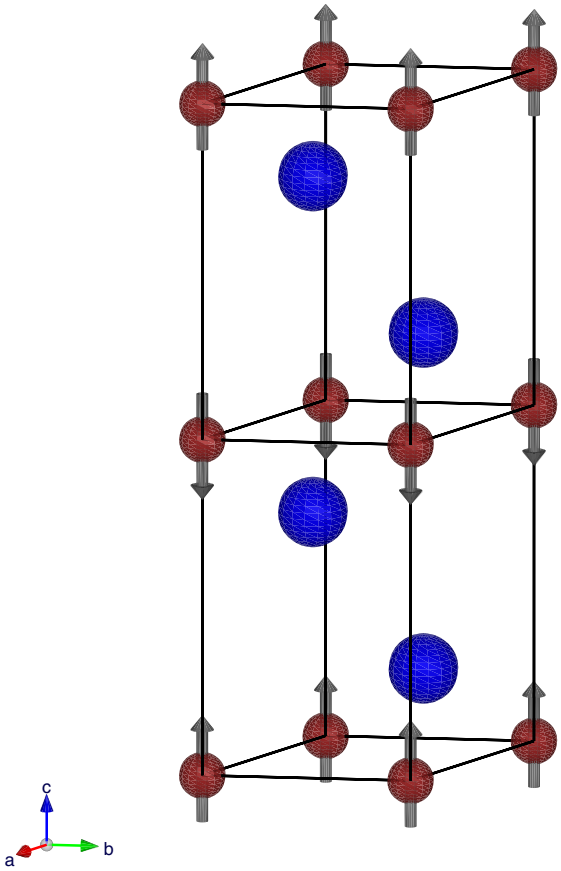

Figure 1. Antiferromagnetic ordering for crystal structure of $FeBr_2$. The ferromagnetic iron layers are perpendicular to the hexagonal c-axis. The large and small balls indicate the Br and Fe atoms, respectively.

2. Computational methods

$FeBr_2$ structure type is of hexagonal layered CdI_2 type (space group $p\bar{3}m1$, No. 164 in international tables [10]) with experimental lattice parameters $a = 7.13$ and $c = 11.76$ Bohr radii. If the iron atom is located at (0,0,0), the coordinates of the two bromine atoms are $\pm(1/3, 2/3, 1/4)$. The hexagonal layer of Fe cations is sandwiched (Br–Fe–Br) by similar (but displaced) layers of Br above and below, with Fe–Br layer spacing such that the Fe ion is surrounded by a nearly perfect bromine octahedron with an 54.47° rotation around the c axis at ambient pressure. The Fe–Br distance in $FeBr_6$ octahedra is 5.05 Bohr radii. As the compound has an AFM ground state with FM iron sheets, we doubled the Bravais lattice unit cell along the c axis using two Fe atoms and four Br atoms per supercell, as shown in figure 1.

To determine the magnetic properties of $FeBr_2$, the four-component Kohn–Sham–Dirac (KSD) equation in the framework of density functional theory [11], which implicitly contains spin–orbit coupling up to all orders, is solved self-consistently. We use the relativistic version of the full-potential local orbital method (FPLO) [12, 13]. The full Brillouin zone was sampled with regular mesh containing 12 × 12 × 6 k-points. The Perdew–Wang parameterization [14] of the exchange–correlation (XC) potential in the local spin-density approximation was used. In this method, the following minimum basis set was adopted: the 3s3p; 4s4p3d states of Fe and the 3s3p; 4s4p states of Br were treated as valence states. The inclusion of Fe and Br 3s 3p semicore states was necessary to account for the non-negligible core–core overlap. The site-centered potentials and densities were expanded in spherical harmonic contributions up to $l_{\max} = 12$. The spatial extension of the basis orbitals, controlled by a confining potential $(r/r_0)^4$, was optimized to minimize the total energy. A major advantage of this potential is that the far ranging tails of these valence orbitals are compressed, which enhances the suitability of the states for the band structure calculations.

In the LSDA for BCC Fe, magnetic spin moments are obtained typically within 5% of experiment. On the other hand, the orbital moment of BCC Fe is found to be a factor of 2 smaller compared with the experimental value (0.08 μ_B) in this approach [15]. For a better description of orbital magnetism in the d shell of the Fe atom, different OP corrections to the LSDA have been suggested.

OP corrections for the unfilled Fe 3d subshell states were included in the orthogonal formalism and as far as possible derived from KSD theory by Eschrig *et al* [16–18]. The correction is added to the LSDA exchange and correlation energy functional:

$$E_l^{\mathrm{OPE}} = -\tfrac{1}{4}\sum_{\sigma} p_l N_\sigma (2l + 1 - N_\sigma) M_{l\sigma}^2, \qquad (1)$$

$$M_{l\sigma} = \sum_{k,m} n_k \langle \psi_k | \varphi_{m\sigma} \rangle m \langle \varphi_{m\sigma} | \psi_k \rangle, \qquad (2)$$

where $M_{l\sigma}$ are the orbital moments of the Fe 3d spin subshells. $N_\sigma = \sum_k n_k |\langle \psi_k | \varphi_{m\sigma} \rangle|^2$, and $\sigma = \uparrow (\downarrow)$ denotes the majority (minority) spin direction. The variables n_k, ψ_k, and $\varphi_{m\sigma}$ are occupation numbers, KSD bispinor orbitals and scalar local l basis functions, respectively. The l and m denote azimuthal and magnetic quantum numbers. The coefficient p_l increases linearly within a shell. The value of the coefficient p_l, which is calculated for free iron ions (Fe^{2+}) is 57.6 meV [16]. In order to compare our results with a frequently employed empirical OP correction suggested by Eriksson *et al* [19] in a spin dependent form for incompletely filled d shells, we alternatively added a term $E_l^{\mathrm{OPB}} = -\sum_\sigma B_{l\sigma} M_{l\sigma}^2/2$ to the XC energy functional. Here, $B_{l\sigma}$ is the related Racah parameter and calculated from the Fe 3d radial wavefunctions. The final values of spin and orbital moments are obtained from corresponding projections on the atom basis states.

We also compare our calculated spin and orbital moments with other existing methods. We completed a series of LSDA + U calculations in its two implementations: the atomic limit (AL) and around mean field (AMF). Although, for transition metal ions, the d orbitals are assumed to be well localized, and therefore best described by the atomic limit extension of LSDA + U, for the sake of completeness, we also added a study with AMF [20–22]. Relativistic LSDA + U electronic structure calculations were performed using the WIEN2k code [24, 25], which implements the full-potential linearized augmented plane-waves (LAPW) method with local orbitals. The spin–orbit interaction (assuming (001) direction

of magnetization) was included within the second variation step method (see [23] and references therein). Radii of atomic spheres were set to 2.8 Bohr radii for both atomic spheres. The Brillouin zone (BZ) was sampled on a regular set of $12 \times 12 \times 6$ k-points in the full BZ, leading to 100 k-points in the irreducible wedge of the first BZ. We performed numerical tests for up to 5000 k-points in the BZ to ensure that our results converged well with respect to BZ sampling. The $RK_{\max}$ parameter for controlling the basis size was set to 7.5, giving more than 100 basis functions per atom and leading to highly converged results. The Fe 3d orbitals were taken to be the correlated orbitals. For the sake of comparison, the same Slater parameters were used for all calculations. The Hund's rule exchange $J^{\mathrm{H}} = (F^2 + F^4)/14 = 0.9$ eV and the ratio $F^4/F^2 = 0.625$ are close to ionic values [25], which leads to $F^2 = 7.9$ eV and $F^4 = 5.0$ eV. The parameter $F^0 = U$ is less well-known since it is more affected by screening effects. We used a literature value for $U = 6$ eV [25].

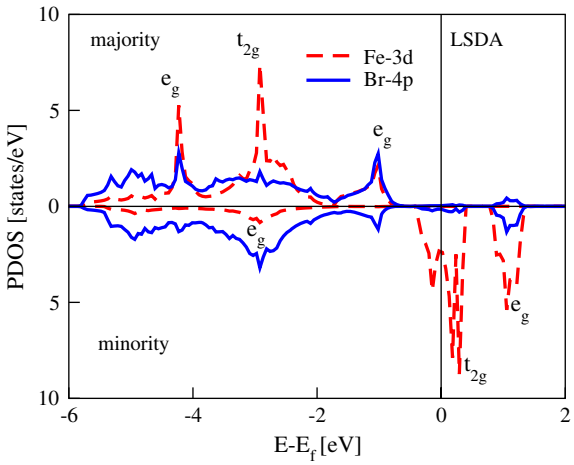

Figure 2. Partial density of states of Fe 3d and Br 4p of $FeBr_2$ states in the framework of the LSDA.

3. Results and discussion

The d electrons of iron and p electrons of bromide ions determine the magnetic behavior of $FeBr_2$. In a fully ionic picture the Fe^{2+} ions are in a $3d^6$ configuration while Br^- ions have a $4p^6$ configuration. Therefore, based on Hund's rules, the quantum numbers of Fe^{2+} would be $S = 2$ and $L = 2$, while both are zero for Br^-. These quantum numbers for $FeBr_2$ yield the ground state ^{4}D, with a total magnetic moment $\mu = 6\mu_{\mathrm{B}}$ on the Fe site and no magnetic moment in the Br site.

In a slightly different view of the structure of $FeBr_2$, as the Fe ions are surrounded by slightly distorted bromine octahedra, the positions of the octahedra lead to a new natural basis for Fe 3d orbitals. In the local coordinate system for every octahedron, in which the z axis is pointed to one of the bromine ions (there is no apical bromine) and the x and y axes are directed to the basal plane bromines, a regular octahedron of Br^- ions produces a ligand field which splits the Fe 3d manifold into three lower lying t_{2g} states (d_{xy}, d_{xz}, and d_{yz}) and two e_g states ($d_{x^2-y^2}$, and $d_{3z^2-r^2}$) of higher energy. Also the Br 4p states are split into σ levels, the orbitals of which point to the Fe site and into π levels and they are perpendicular to the Fe–Br bonds. This ligand field provides a splitting resulting from the hybridization between the Fe e_g states and Br 4p orbitals. The hybridization is strongest for the σ bonds between in-plane Fe $3d_{x^2-y^2}$ and in-plane Br $4p_{x,y}$ orbitals, which leads to bonding σ and anti-bonding σ^* Fe $3d_{x^2-y^2}$-Br $4p_{x,y}$ covalency states. The formation of the lower lying σ bonding states results in the wide 4p band, whereas the e_g bond energy is raised by the anti-bonding. In between these bands there are other bands formed from hybrids which have a smaller splitting between bonding and anti-bonding states. Figure 2 shows partial density of states for Fe 3d and Br 4p of $FeBr_2$. It can be seen that the e_g-density of states (DOS) and p manifold of both spin channels imply a strong p e_g hybridization, while no such feature is observed for the t_{2g}-DOS. Therefore, the p t_{2g} hybridization can be neglected.

In the ligand field interaction picture, it is easy to show that the orbital moments are completely quenched. To illustrate this argument we consider a simplified model of a 3d transition metal ion in the perfect octahedral ligand field (for a comprehensive discussion see the textbook by Figgis *et al* [26]). Neglecting the spin-flip process, we consider only one partially filled spin subshell. The three-fold degenerate t_{2g} and two-fold degenerate e_g states can be represented by real d-functions with $\{|xy\rangle, |xz\rangle, |yz\rangle\} = \{(|{+2}\rangle - |{-2}\rangle)/\mathrm{i}\sqrt{2}, (|{+1}\rangle - |{-1}\rangle)/\mathrm{i}\sqrt{2}, (|{+1}\rangle + |{-1}\rangle)/\sqrt{2}\}$, and $\{|x^2 - y^2\rangle, |3z^2 - r^2\rangle\} = \{(|{+2}\rangle - |{-2}\rangle)/\sqrt{2}, |0\rangle\}$, respectively. The $|m\rangle$ means the 3d-orbital with magnetic number. It is obvious that the expectation value of the orbital moment is zero for each eigenfunction of the ligand Hamiltonian and therefore the total orbital moment of the 3d-subshell is completely quenched.

Disregarding spin–orbit coupling, the direction of spin is not related to the real space and the resulting doubled antiferromagnetic primitive cell has rhombohedral symmetry. This allows a further splitting of the t_{2g} manifold into two-fold degenerate e_g' and non-degenerate a_{1g} states (closed bumps shown in figure 2 originate from further splitting of t_{2g} states in majority and minority partial DOS). In both spin channels e_g and t_{2g} bands are well separated for all momenta. The LSDA result for the t_{2g} and e_g bandwidths is 0.6 eV, and the ligand field splitting of the centroids of these bands is about 0.6 eV. Thus the exchange splitting (about 2 eV) is larger than the ligand field splitting, which is a consequence of the ferromagnetic phase on the iron sheets. The calculated spin and orbital magnetic moments of Fe and Br for [001] magnetization axes are summarized in table 1. The LSDA gives spin moments of 3.49 and 0.17 μ_{B}/atom for Fe and Br, respectively. In the ligand field model, one can estimate that both t_{2g} and e_g orbitals of the majority Fe-d bands are fully occupied, and only one of the minority t_{2g} orbitals is occupied. Therefore, the spin contribution to the total magnetic moment of an Fe atom from the DOS study is 4 μ_{B}. However, the LSDA calculated spin moment of Fe is smaller than the value estimated in the ligand field model by about 12%. The spin moment of the Fe atoms is parallel to that of the Br atoms. The orbital moment of the Br atoms is almost negligible compared with that of the spin

moment. The orbital moment of Fe is also parallel to the spin moment of Fe, being consistent with Hund's rules for 3d shells more than half-filled. Hence the resultant magnetic moments of Fe and Br are ferromagnetically coupled in $FeBr_2$.

An interesting question is the origin of the small orbital moment on an Fe ion ($\mu_l = 0.14\ \mu_B$) in the presence of spin–orbit coupling in our LSDA calculation. As we have seen, the small lattice distortion modified the electronic structure insignificantly, provided that the symmetry of the structure is not changed. However, due to the action of spin–orbit coupling on the Fe ions, a small deviation of the nearest-neighbor octahedra can be expected, which lacks the perfect octahedral symmetry, resulting in new states. In this new picture the origin of the small orbital moment may be understood.

In our LSDA + U calculations, with the literature values of $U = 6$ eV and $J^H = 0.9$ eV and in the framework of LAPW, the spin moments of Fe increased by 6% and 0.2% for AL (3.70 μ_B) and AMF (3.50 μ_B) approaches, while the spin moment of Br reduced by 58% and 17%, respectively. Meanwhile, the orbital moment of Fe increases dramatically by a factor of about four (AL) and five (AMF) compared with the LSDA value (see table 1). Note that increasing U reduces the total charges in the Fe muffin-tin spheres and increases the total charges in the Br muffin-tin spheres, thus increasing the ionicity of both the Fe and Br atoms. In the LSDA, the unquenched orbital moment arises mainly from the spin–orbit interaction in the localized 3d orbital where the atomic field is deformed in a relatively slight manner by the ligand field. The strong Coulomb correlations further localize the 3d orbitals and suppress the ligand field on the metal atoms. This compound is thus expected to possess relatively large unquenched orbital moments. Although the calculated orbital moments from the LSDA are usually too small compared with experimental results, the on-site Coulomb energy U in both LSDA + U^{AL} and LSDA + U^{AMF} calculations significantly enhances the orbital moment on the Fe site at $FeBr_2$, and gives large orbital moments 0.75 and 0.66 μ_B, respectively.

We have also included in our study on orbital magnetism of $FeBr_2$ the results of two OP corrections. Table 1 shows the results of both OP corrections for spin and orbital contributions to the magnetic moments of the Fe atom in $FeBr_2$. As is usually the case, OP corrections influence the spin moments only marginally. However, the calculated orbital moments of Fe in both OPB (0.43 μ_B) and OPE (0.60 μ_B) schemes are three and four times larger than the LSDA calculated value (0.14 μ_B). We also found that the orbital moment of Fe 3d within the OPE correction is roughly in good agreement with LSDA + U^{AL} calculations. One may also compare the orbital moment evaluated with an OPB correction, which is smaller than the calculated value of LSDA + U^{AL} by about 35%.

Ropka *et al* have shown in their quasiatomic calculations that the orbital moment of Fe is 0.78 μ_B [7]. Meanwhile, Youn *et al* using the full relativistic full-potential linear muffin-tin orbital (LMTO) method in combination with the LSDA + U approach have shown an orbital moment of 0.66 μ_B/Fe [8]. These findings are in qualitative agreement with our results. On the other hand, our calculated spin magnetic moments of iron in the considered compound are smaller by about 20% than the experimental value estimated by Wilkinson *et al* [6] in their neutron diffraction investigations. In this sense, adding a large orbital contribution to the spin magnetic moment modifies the total magnetic moment of iron such that it becomes consistent with the experimental value (see table 1).

Table 1. Calculated spin magnetic moment (μ_s) and orbital magnetic moments (μ_l) of iron and bromine and total magnetic moment of iron $\mu = \mu_s + \mu_l$. The magnetic moments are in Bohr magnetons.

	μ_s^{Fe}	μ_l^{Fe}	μ^{Fe}	μ_s^{Br}
LSDA	3.49	0.14	3.63	0.17
LSDA + U^{AMF}	3.50	0.75	4.25	0.14
LSDA + U^{AL}	3.70	0.66	4.36	0.07
LSDA + OPB [19]	3.57	0.43	4.00	0.20
LSDA + OPE [16]	3.58	0.60	4.18	0.20
Expt [6]			4.4 ± 0.7	

In LSDA band structure calculations, correlation and exchange effects are taken into account within approximation of a homogeneous electron liquid. Within this model, an intermetallic state takes place in contradiction with the nature of the antiferromagnetic insulator of $FeBr_2$ with a gap of about 2 eV [8]. Therefore we note that our LSDA calculations do not give correct results for the gap size of $FeBr_2$, exhibiting qualitatively erroneous non-zero DOS at the Fermi level (see figure 2). Both OP corrections also predict, however, an intermetallic ground state. In $FeBr_2$, the 3d electrons are strongly localized at the Fe site and hop from time to time from one site to the next. In this case, the Coulomb interaction, U, between two holes (or two electrons) on the same site will be important and may be the reason for the insulating behavior of the compound. This point was discovered by Youn *et al* [8], in their LMTO study.

4. Conclusions

Density functional theory calculations were performed for the antiferromagnetic insulator $FeBr_2$. We have calculated the spin and orbital moments of individual components of $FeBr_2$, including spin–orbit coupling, and two variants of LSDA + U and two variants of orbital polarization corrections. The large orbital moment for iron ions varies with different methods from 0.43 μ_B to 0.70 μ_B. We also found a small amount of spin magnetic moment for the Br ion. Further experiments, such as x-ray magnetic circular dichroism, to check these predictions are desirable.

Acknowledgments

We are grateful to Dr Manuel Richter and Dr Kris Delaney for many useful discussions. Financial support by Deutsche Forschungsgemeinschaft, SPP 1145, and hospitality of the Leibniz Institute for Materials Research and Solid State Physics (IFW), Dresden, Germany are gratefully acknowledged. The work of JR was supported by the STINT, the Swedish Research Council, and the Foundation for Strategic Research.

References

[1] Ito A and Di N L 1999 *J. Phys. Soc. Japan* **68** 1098
[2] Aruga Katori H, Katsumata K and Katori M 1996 *Phys. Rev.* B **54** 9620
[3] Stryjewski E and Giordano N 1977 *Adv. Phys.* **26** 487
[4] Yelon W B and Vettier C 1975 *J. Phys. C: Solid State Phys.* **8** 2760
[5] Pelloth J, Brand R A, Takele S, Pereira de Azevedo M M, Kleemann W, Binek Ch, Kushauer J and Bertrand D 1995 *Phys. Rev.* B **52** 15372
[6] Wilkinson M K, Cable J W, Wollan E O and Koehler W C 1959 *Phys. Rev.* **113** 497
[7] Ropka Z, Michalski R and Radwanski R J 2001 *Phys. Rev.* B **63** 172404
[8] Youn S J, Sahu B R and Kim K S 2002 *Phys. Rev.* B **65** 052415
[9] Richter M 2001 Density functional theory applied to 4f and 5f elements and metallic compounds *Handbook of Magnetic Materials* vol 13, ed K H J Buschow (Amsterdam: North-Holland) pp 87–228
[10] Villars P and Calvert L D 1991 *Pearson's Handbook of Crystallographic Data for Intermetallic Phases* 2nd edn (Metals Park, OH: ASM International)
[11] Hohenberg P and Kohn W 1964 *Phys. Rev.* **136B** 864
[12] Koepernik K and Eschrig H 1999 *Phys. Rev.* B **59** 1743 http://www.FPLO.de.
[13] Opahle I 2001 *PhD Thesis* Technische Universität Dresden
Eschrig H, Richter M and Opahle I 2004 Relativistic solid state calculations *Relativistic Electronic Structure Theory—Part II: Applications* ed P Schwerdtfeger (Amsterdam: Elsevier) pp 723–76
[14] Perdew J P and Wang Yu 1992 *Phys. Rev.* B **45** 13244
[15] Brooks M S S 1985 *Physica* B **130** 6
[16] Eschrig H, Sargolzaei M, Koepernik K and Richter M 2005 *Europhys. Lett.* **72** 611
[17] Sargolzaei M 2006 *PhD Thesis* Technische Universität Dresden
[18] Sargolzaei M, Richter M, Koepernik K, Opahle I, Eschrig H and Chaplygin I 2006 *Phys. Rev.* B **74** 224410
[19] Eriksson O, Johansson B and Brooks M S S 1989 *J. Phys.: Condens. Matter* **1** 4005
[20] Czyżyk M T and Sawatsky G A 1995 *Phys. Rev.* B **49** 14211
[21] Eschrig H, Koepernik K and Chaplygin I 2003 *J. Solid State Chem.* **176** 482
[22] Chaplygin I 2002 *PhD Thesis* Technische Universität Dresden
[23] Blaha P, Schwarz K, Madsen G K H, Kavsnicka D and Luitz J 2001 *Computer Code WIEN2k* Technische Universität Wien, Wien
[24] Anisimov V I, Zaanen J and Andersen O K 1991 *Phys. Rev.* B **44** 943
[25] Anisimov V I, Solovyev I V, Korotin M A, Czyżyk M T and Sawatzky G A 1993 *Phys. Rev.* B **48** 16929
[26] Figgis B N and Hitchman M A 2000 *Ligand Field Theory and its Applications* (New York: Wiley–VCH)